Quantitative analysis of the first-principles effective Hamiltonian approach to ferroelectric perovskites

Silvia Tinte, Jorge Íñiguez, Karin M. Rabe, and David Vanderbilt
Department of Physics and Astronomy, Rutgers University, Piscataway, New Jersey 08854-8019
(Received 21 October 2002; published 27 February 2003)

The various approximations used in the construction of a first-principles effective Hamiltonian for $BaTiO_3$, and their effects on the calculated transition temperatures, are discussed. An effective Hamiltonian for $BaTiO_3$ is constructed not from first-principles calculations, but from the structural energetics of an atomistic shell model for $BaTiO_3$ of Tinte *et al.* This allows the elimination of certain uncontrolled approximations that arise in the comparison of first-principles effective Hamiltonian results with experimental values and the quantification of errors associated with the selection of the effective Hamiltonian subspace and subsequent projection. The discrepancies in transition temperatures computed in classical simulations for this effective Hamiltonian and for the atomistic shell model are shown to be associated primarily with a poor description of the thermal expansion in the former case. This leads to specific proposals for refinements to the first-principles effective Hamiltonian method. Our results suggest that there are at least two significant sources of error in the effective-Hamiltonian treatment of $BaTiO_3$ in the literature, i.e., the improper treatment of thermal expansion and the errors inherent in the first-principles approach itself.

DOI: 10.1103/PhysRevB.67.064106 PACS number(s): 77.80.Bh, 77.84.Dy, 77.80.−e

I. INTRODUCTION

First-principles methods constitute a powerful tool for the study of ferroelectric systems.[1] Ground state structures, phonons, spontaneous polarization, and related properties, including piezoelectric and dielectric tensors, have been accurately calculated for a wide variety of perovskite oxides as well as other ferroelectric compounds.

Despite advances in algorithms and computer hardware, the direct calculation of finite temperature behavior, particularly phase transitions, is still far beyond reach, as such calculations involve thousands of atoms. However, indirect methods have been developed and applied to a large number of systems, including $BaTiO_3$,[2–4] $PbTiO_3$,[5] and $KNbO_3$,[6,7] and even solid solutions such as $Pb(Zr_xTi_{1-x})O_3$,[8,9] $Pb(Sc_{0.5}Nb_{0.5})O_3$,[10] and $K(Nb_xTa_{1-x})O_3$.[11] In Refs. 4, 6, and 11, interatomic ''shell-model'' potentials were parametrized by fitting to first-principles results, and finite-temperature behavior studied by direct simulation of atomistic systems with forces and energies obtained from these potentials. The results in Refs. 2, 3, 5, and 7–10 were obtained by an effective Hamiltonian construction in which the full system is mapped by a subspace projection onto a statistical mechanical model, with parameters determined from first-principles calculations of total energies for small distortions of an ideal crystal with the cubic perovskite structure. The simple form of the resulting effective Hamiltonian allows very-large-scale simulations and aids in the conceptual interpretation of the results. The two approaches have achieved comparable success in reproducing many essential features of the phase transitions of ferroelectrics. For example, for $BaTiO_3$,[2–4] the experimentally observed cubic-tetragonal-orthorhombic-rhombohedral phase sequence is correctly reproduced. However, while the experimental values of the transition temperatures are 403, 278, and 183 K, classical Monte Carlo simulations of the first-principles effective Hamiltonian give 300, 230, and 200 K, while the shell-model results are 210, 135, and 100 K, respectively. In both cases a correction for the local-density approximation (LDA) lattice constant underestimate was included in the model.

Understanding the origin of this discrepancy with experiment may help in the development of improved theoretical methods for the calculation of finite temperature behavior. Here, we focus our attention on the first-principles effective Hamiltonian approach. The discrepancies in the transition temperatures could result from separate errors introduced at various steps of the analysis. We correspondingly classify the errors into five types. Errors in the configuration energies obtained from first-principles calculations will be designated type I. These generally can be systematically reduced, with the exception of the uncontrolled approximation in the exchange-correlation functional required for the practical implementation of density functional theory (''LDA error''). Type II errors result from the identification of the relevant degrees of freedom and the projection and approximate representation of the effective Hamiltonian in the corresponding subspace, and will be the main focus of our investigation. Errors in the statistical-mechanical simulations (type III) include finite-size effects and sampling errors. In the effective Hamiltonian studies to date, it has been feasible to make these errors relatively negligible. The importance of type IV errors, resulting from the classical treatment of the ions neglecting quantum fluctuations, has been highlighted in a recent study of $BaTiO_3$ by Íñiguez and Vanderbilt.[12] The results of this study indicate that the classical approximation *raises* the transition temperatures. Thus, this is not the origin of the underestimate for $BaTiO_3$. In fact, a correct, fully quantum-mechanical treatment would increase, not decrease, the transition-temperature discrepancy. Finally, we note that the experimental samples, even in thermodynamic equilib-

rium, contain defects and local nonstoichiometry which lead to deviations of observed properties from those of the assumed ideal crystals (type V errors). These crystal imperfections can have various effects on the transition temperatures that are in general difficult to model.

To separate and quantify the role of the various errors in producing the observed discrepancies in transition temperatures, several different approaches could be applied. The analysis of type III and type IV errors has been discussed in the previous paragraph. One way to investigate type I errors would be completely to redo the effective Hamiltonian study replacing the LDA with a generalized-gradient approximation (GGA). However, the latter has not been found to give systematic improvement in the overall agreement of calculated properties with experiment,[13] and thus the value of such a labor-intensive investigation is unclear. In principle, type II errors could be eliminated by comparing the effective-Hamiltonian transition temperatures with those obtained in a fully *ab initio* molecular dynamics or Monte Carlo calculation. However, as noted above, doing this type of direct calculation for sufficiently large systems is so computationally demanding that it is impossible in practice even for benchmarking purposes, and calculations for small supercells and with reduced sampling would introduce significant finite-size and statistical errors.

In this paper we develop and carry out an alternative method of isolating and quantifying type II errors, allowing us to discuss possible refinements of the effective Hamiltonian method to reduce or eliminate them. We use the total energies computed with the $BaTiO_3$ ''shell model'' interatomic potential of Tinte *et al.*[4] to construct an effective Hamiltonian, and compare the computed transition temperatures with those obtained in direct classical simulations for the ''shell model'' system. In this comparison, we completely eliminate errors of types I, IV, and V, and can easily make errors of type III negligible. Thus, we can attribute any discrepancies directly to errors of type II. While such errors will not be quantitatively identical to the corresponding errors made in the construction of the effective Hamiltonian directly from *ab initio* results, the general accuracy and physical faithfulness of the shell model interatomic potential to $BaTiO_3$ should render conclusions based on this analysis quite meaningful.

The paper is organized as follows. Section II provides technical details of the $BaTiO_3$ shell-model interatomic potential of Tinte *et al.* that serves as our reference system. In Sec. III we describe the construction of the effective Hamiltonian and the parameters obtained by fitting to the shell model, paying special attention to the approximations and technicalities involved. In Sec. IV we present the results obtained from the effective-Hamiltonian and shell-model classical statistical-mechanical simulations. The discrepancies are analyzed in Sec. V, and possible improvements on the various effective-Hamiltonian approximations are discussed. Section VI is devoted to the specific issue of modeling the thermal expansion within the effective-Hamiltonian approach. Finally, in Sec. VII we present a discussion of the broader implications of our analysis; in particular, we speculate on the relative importance of errors of types I, II, and IV in the first-principles effective-Hamiltonian treatments currently in the literature.

II. SHELL-MODEL INTERATOMIC POTENTIAL

Of the various types of interatomic potentials, shell models are uniquely well suited to giving a good description of the lattice dynamics of perovskite oxides. The form of the shell-model potential developed for $BaTiO_3$ in Ref. 4 incorporates earlier observations that the oxygen shell-core interaction should be nonlinear and anisotropic.[14,15] Each ion (Ba, Ti, or O) is modeled as a massive core linked to a massless shell. The core-shell interactions for Ba and Ti are harmonic and isotropic. An anisotropic core-shell interaction is considered at the O^{-2} ions, with a fourth-order core-shell interaction along the O-Ti bond. In addition to the Coulomb interactions between ion cores and shells, the model contains pairwise short-range intershell potentials of the Buckingham type, i.e., $V(r)=a\exp(-r/\rho)-c/r^6$. The Born-Mayer form ($c=0$) is sufficient for the Ti-O and Ba-O short-range potential, while for the O-O potential the value of c is nonzero. The physically important nonlinearities of the interatomic interactions are thus naturally incorporated into the form of the potential.

The material-specific parameters in the interatomic potential were determined by adjusting them to fit selected first-principles results computed using the linearized augmented planewave (LAPW) method as discussed in detail in Ref. 4. It should be noted, however, that the equilibrium lattice constant of the cubic phase is fitted to the experimental cubic-phase lattice constant extrapolated to 0 K (3.995 Å), not the LAPW lattice constant. The double wells for polar distortions along (001), (011), and (111) are satisfactorily reproduced, as are the phonon dispersion curves for the cubic structure at the experimental lattice constant. The bulk modulus of the cubic phase and the anomalous Born effective charges are also in good agreement with the first-principles results. Reference 4 contains further details about the construction of the interatomic potential and values of the parameters.

Finite-temperature properties of the system described by this interatomic potential are investigated by constant-pressure molecular dynamics (MD) simulations using the DL-POLY package,[16] where the adiabatic dynamics of the electronic shells are approximated by assigning small masses to them. A Hoover constant-$(\bar{\sigma},T)$ algorithm with external stress set to zero is employed; all cell lengths and cell angles are allowed to fluctuate. The time step is 0.4 fs and the total time of each simulation, after 2 ps of thermalization, is 20 ps. Results for a $7\times7\times7$ periodic supercell (1715 ions plus 1715 shells which are additional degrees of freedom) were reported in Ref. 4. It was shown that the cubic-tetragonal-orthorhombic-rhombohedral phase sequence is correctly reproduced. Good agreement with experimental data was obtained for the structural parameters in the various phases as well as the volume thermal expansion coefficient, showing that the most important nonlinearities have been included in the model. However, the transition temperatures are rather low compared to experiment (190, 120, and 90 K). This dis-

crepancy does not affect the present analysis of type II errors. In the present work, we have expanded the supercell to $10\times10\times10$ primitive cells (10 000 degrees of freedom). This yields essentially the same results, except that the calculated transition temperatures increase slightly (210, 135, and 100 K). Additional MD simulations were performed at constant volume, using a modified Hoover constant-$(\overline{\sigma},T)$ algorithm that allows for fluctuations in the cell shape.

III. CONSTRUCTION OF THE EFFECTIVE HAMILTONIAN

In this section we describe the effective Hamiltonian that we have constructed using the shell model for $BaTiO_3$ of Tinte *et al.*[4] as our target system. The form of the effective Hamiltonian is identical to that proposed by Zhong *et al.*,[3] except that the inhomogeneous strain variables found to be unimportant in that study are not included here.

An effective Hamiltonian is a Taylor expansion of the energy surface of the system around a high-symmetry phase in terms of a set of relevant degrees of freedom. For ferroelectric perovskites, the most convenient reference structure is the cubic paraelectric phase. The relevant degrees of freedom can be identified by studying the energy changes induced by small (harmonic) perturbations of the reference structure. The low-energy, typically unstable, distortions are the relevant ones, and are expressed in the form of local modes or lattice Wannier functions.[17] The relevant local modes are those that add up to produce the distorted ferroelectric ground-state structure. Also, we take the homogeneous strains as relevant and include them in the Hamiltonian.

There are two possible ways of performing the harmonic analysis that leads to the identification and calculation of the relevant lattice Wannier functions. One can study either the force-constant matrix (the matrix of second derivatives of the energy with respect to atomic displacements) or the corresponding dynamical matrix. While the former choice leads to a better description of the lowest-energy states of the system, the latter provides a kinetic decoupling between the relevant and *irrelevant* (i.e., not considered in the Hamiltonian) degrees of freedom. Here we have worked with the force-constant matrix, which is more appropriate for the study of equilibrium properties. In any case, we find numerically that the force constant and dynamical matrix descriptions are essentially identical.

Once a relevant set of phonon branches[18] has been identified, the calculation of the corresponding lattice Wannier functions can be done at different levels of approximation. At the crudest level, they can be constructed from phonons at a single k point,[3] more sophisticated schemes allowing for better descriptions of the relevant phonons throughout the Brillouin zone.[17,19] Here, we calculate the local modes from the unstable phonons at Γ, which generate the ferroelectric structure, choosing the local modes to be centered on the Ti atom. The resulting local modes reproduce the unstable phonons at zone-boundary points M and X with an accuracy above 97%. We thus do not expect a better local-mode definition to constitute a significant improvement of our effective Hamiltonian of shell-model $BaTiO_3$.

TABLE I. Expansion parameters of the effective Hamiltonian fitted to the shell-model $BaTiO_3$ target system. The notation is taken from Ref. 3. All the parameters are in atomic units.

On-site	κ_2	0.0562	α	0.805	γ	−0.849
Intersite	j_1	−0.01424	j_2	−0.01506		
	j_3	0.00422	j_4	−0.00240	j_5	0.01956
	j_6	0.00100	j_7	0.00050		
Elastic	B_{11}	5.42	B_{12}	2.06	B_{44}	2.07
Coupling	B_{1xx}	−4.16	B_{1yy}	−1.19	B_{4yz}	−0.44
Dipole	Z^*	8.153	ϵ_∞	5.24		

Let $u_{i\alpha}$ denote the local mode amplitude in unit cell i along Cartesian direction α. Let η_l denote the strains, where l is a Voigt index. Our effective Hamiltonian can then be written as

$$H_{\rm eff}=E^{\rm self}[u_{i\alpha}^2;u_{i\alpha}^2u_{i\beta}^2]+E^{\rm dpl}[u_{i\alpha}u_{j\beta}]+E^{\rm short}[u_{i\alpha}u_{j\beta}]+E^{\rm elas}[\eta_l\eta_m]+E^{\rm int}[\eta_l u_{i\alpha}u_{i\beta}]. \quad (1)$$

Following Ref. 3, we have written the effective Hamiltonian as the sum of four terms: the on-site self-energy of the local modes $E^{\rm self}$, the long-range dipole-dipole interactions between local modes $E^{\rm dpl}$, the short-range interactions between local modes $E^{\rm short}$, the elastic energy $E^{\rm elas}$, and the interaction between local modes and strains $E^{\rm int}$. The dependence of each term on the model variables is indicated in Eq. (1). It should be noted that the form of the Hamiltonian is greatly simplified by the cubic symmetry of the reference structure. For example, there are no odd terms in $u_{i\alpha}$.

The relevant phonon branches are described by the harmonic terms in $E^{\rm self}$, $E^{\rm dpl}$, and $E^{\rm short}$. Anharmonic terms for the local modes, required to stabilize the low-symmetry phases, are included only in $E^{\rm self}$ (the ''local-anharmonicity approximation''). In both $E^{\rm elas}$ and $E^{\rm int}$ only the lowest-order terms in the expansion are considered. This constitutes the minimal microscopic model for the description of ferroelectricity in $BaTiO_3$. Including higher-order terms in the Hamiltonian would constitute a systematic improvement of the model.

As already mentioned, the Hamiltonian we have just described is essentially that of Ref. 3, except the parameters were fitted to a series of shell-model calculations of total energies and forces, instead of *ab initio* results, for a set of distorted structures. The minimum-energy cubic structure of the shell model is taken as the reference structure, so that both share the same relaxed cubic lattice constant. Following the notation of Ref. 3, we list in Table I the parameters defining our effective Hamiltonian for shell-model $BaTiO_3$.

Monte Carlo (MC) simulations were performed to calculate the finite-temperature properties of the Hamiltonian. We simulated a $10\times10\times10$ supercell with periodic boundary conditions, and typically did 30 000 MC sweeps to equilibrate the system and 50 000 sweeps more to obtain averages

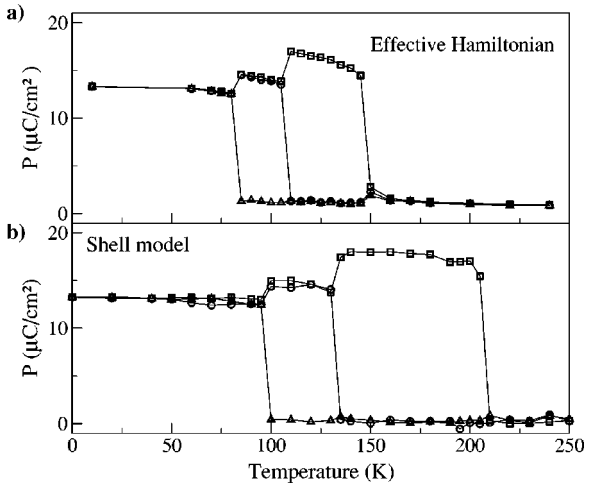

FIG. 1. Behavior of three Cartesian components of the mean (supercell averaged) polarization of $BaTiO_3$ as obtained from (a) MC simulations using the effective Hamiltonian and (b) MD simulations directly from the shell model.

of local-mode variables with a statistical error below 10%. The temperature was increased in small steps of 5 K.[20] We monitored the behavior of the homogeneous strain and the vector order parameter to identify the transitions. The average local-mode vector is proportional to the polarization. Note that, unless it is indicated, the MC simulations for the present effective Hamiltonian are performed at zero external pressure.

IV. FINITE-TEMPERATURE RESULTS

Figure 1(a) shows the three components of the mean polarization as a function of temperature as obtained from the MC simulations of the effective Hamiltonian, while Fig. 1(b) shows the corresponding results obtained directly from the shell-model MD simulations. It is apparent that the effective Hamiltonian correctly reproduces the sequence of transitions (cubic to tetragonal to orthorhombic to rhombohedral with decreasing T). However, the agreement is far from perfect for the T_c values, listed in Table II. Clearly the effective Hamiltonian underestimates the T_c's, especially for the $C-T$ transition where the transition temperature is too low by $\sim 30\%$.

TABLE II. $BaTiO_3$ transition temperatures, in K, between cubic (C), tetragonal (T), orthorhombic (O), and rhombohedral (R) phases, as obtained from the shell model and from the effective Hamiltonian. The last three rows correspond to effective Hamiltonians modified as indicated in the text. In the first column, percentage error relative to the shell model is given in parentheses.

	$C-T$	$T-O$	$O-R$
Shell model	210	135	100
Effective Hamiltonian	150 (-28%)	110	85
H_{eff} different α and γ	150 (-28%)	120	100
$H_{\text{eff}}+p_{\text{eff}}$ "by hand"	185 (-12%)	125	95
$H_{\text{eff}}+$computed p_{eff}	165 (-21%)	120	90

This shows that for an effective Hamiltonian of this form, type II errors are quite significant, and in fact are comparable to the discrepancies found when comparing $BaTiO_3$ *ab initio* effective-Hamiltonian results against experimental measurements on real $BaTiO_3$ samples. This strongly suggests that errors in first-principles calculations account for at most only part of the latter discrepancy. In the following, we will investigate the type II errors in more detail and identify approaches for the systematic reduction of these errors, returning to the discussion of first-principles effective Hamiltonians in Sec. VII.

V. ANALYSIS OF SOURCES OF THE DISCREPANCIES

In this section, we analyze three sources of error in the construction of the effective Hamiltonian that could possibly lead to the calculated underestimates of the T_c values. First, we focus on the specification of the ferroelectric mode unit vector, which determines the precise set of degrees of freedom described by the effective Hamiltonian. Second, we consider the effect of the truncation of the Taylor expansion in the specified degrees of freedom, with particular attention to the neglect of certain higher-order couplings within the effective Hamiltonian subspace. Third, we consider the consequences of omitting the higher-frequency phonon branches from the effective Hamiltonian.

A. Specification of ferroelectric local mode vector

One of the first choices that was made in the construction of the effective Hamiltonian was the detailed specification of the ferroelectric local mode vector. As explained in Sec. III, we chose a Ti-centered displacement pattern selected in such a way that a uniform superposition of these local mode displacements gives a periodic displacement pattern corresponding to the unstable (ferroelectric) mode eigenvector of the force-constant matrix in the cubic structure. This is only one of many possible approaches, and questions may arise as to whether this is the best choice and how much difference it would make if we had made a different choice.

One way of addressing these questions is to test how completely the chosen local mode vectors span the space of distortions that are actually encountered in the full atomistic finite-temperature shell-model simulation. We projected the shell-model MD trajectories at a given temperature onto the 12 optical zone-center normal modes (i.e., force-constant eigenvectors) of the cubic phase (four sets of threefold degenerate modes). As expected, we found that the mode branches included in our effective Hamiltonian subspace account for almost all ($\sim 90\%$) of the observed atomic displacements. This suggests that the approximation of keeping only these modes in the effective Hamiltonian is a good one.

A second approach is to try a different procedure for defining the identity of the local mode vector. In particular, one could think of a construction designed to optimize the description in the neighborhood of the ferroelectric ground

state. For instance, the local mode vector could be fitted to the ground state of the system that is obtained when the atomic positions are fully relaxed. Such a procedure would effectively incorporate the effect of the anharmonic couplings between included and excluded modes while not increasing the number of variables considered in the model. In order to quantify the effect of this change, we assume that this alternative local mode definition mainly affects the anharmonic parameters in

$$E^{\text{self}} = \kappa_2 u_i^2 + \alpha u_i^4 + \gamma(u_{ix}^2 u_{iy}^2 + u_{iy}^2 u_{iz}^2 + u_{ix}^2 u_{iz}^2). \qquad (2)$$

We thus recalculated α and γ exactly to reproduce the energy of the fully relaxed tetragonal energy minimum, and to get the best compromise for the energies of the orthorhombic and rhombohedral minima. By ''fully relaxed'' we mean that the atomic positions were allowed to relax with the cell constrained to be the equilibrium cubic cell; this is consistent with the fact that we did not recalculate any mode-strain coupling parameter. The new α and γ are 0.811 and -0.916 a.u. respectively, which are very similar to the values in Table I. The smallness of the correction reflects the fact that the fully relaxed energy minima are very close to those described by the original effective Hamiltonian, the differences being of the order of 0.01 mHa. Keeping all other parameters unchanged, we repeated the MC simulations at finite temperature and found that the transition temperatures of the $T-O$ and $O-R$ transitions (see Table II) are sensitive to these small changes in parameter values, giving a 10% improvement compared with our original effective Hamiltonian. However, the large discrepancy in the $C-T$ transition temperature is unchanged.

We therefore conclude that a change in the definition of the local-mode displacement pattern is unlikely to be sufficient to eliminate the discrepancy between the effective-Hamiltonian and shell-model results. It is necessary, therefore, to look elsewhere. Nevertheless, the results do show that the details of the fitting procedure can have a significant effect on the transition temperatures.

B. Neglect of higher-order terms in the Taylor expansion

We now return to our initial choice of relevant degrees of freedom, but ask whether the corresponding energy landscape is sufficiently well described by the truncated Taylor expansion that defines the effective Hamiltonian. The quadratic elastic energy E^{elas} is easily checked to be accurate. Hence, the terms that may require improvement are E^{self}, E^{dpl}, E^{short}, and E^{int}.

Higher-order terms in E^{self} should aim at a better description of the double-well potentials associated with the ferroelectric instabilities. We checked, however, that including sixth- and eighth-order terms does not improve the fit significantly. In particular, the well depths, which are the effective-Hamiltonian feature most directly related to the value of the transition temperatures, are very well reproduced by the quartic E^{self}. A more accurate description would yield energy wells around 1% shallower, which would probably lead to a very tiny decrease in the $C-T$ transition temperature.

Higher-order terms in E^{short} represent anharmonic couplings between neighboring local modes and would provide a correction to the local-anharmonicity approximation. One can fit such terms by looking at the double-well potentials associated with the antiferroelectric instabilities of shell-model $BaTiO_3$ at zone-boundary points X and M. The fourth-order terms associated with such wells will be a combination of the parameters α and γ in Eq. (2) and the new quartic parameters in E^{short}. However, we find that these new quartic parameters are very small and can be safely neglected.[21] More precisely, they constitute 0.05 and 5 % of the total fourth-order term for the X and M instabilities, respectively, and result in slightly deeper zone-boundary energy wells. Their probable effect is a minor decrease in the transition temperatures, because of an enhanced competition between zone-center and zone-boundary instabilities.

The above conclusion about the higher-order terms of E^{short} also applies to those of E^{dpl}, which would manifest themselves in a similar way. Neglecting the higher-order terms of E^{dpl} is essentially equivalent to assuming that the polarization is linear in the atomic displacements, which is a reasonably good approximation for $BaTiO_3$.

One could think of improving on E^{short} by including couplings between further neighbors (following Ref. 3, we included couplings up to third neighbors in our Hamiltonian). This would allow us to improve the description of the dispersion branches of the relevant modes throughout the Brillouin zone. However, we checked that if our Hamiltonian is fitted including couplings only up to second neighbors the transition temperatures change by less than 10 K. Hence, we can assume our Hamiltonian is well converged in this respect.

Finally, the description of the interaction between strain and local modes can be improved by including more terms in E^{int}. In particular, we have found that the $\eta_1 u_{ix}^4$ term is not negligible and would modify the effective Hamiltonian so as to yield higher transition temperatures. Specifically, we find that the coefficient of the $\eta_1 u_{ix}^4$ term is negative and would thus favor a state in which the system polarizes and expands along a Cartesian direction. However, in the next section we will see that the main type II error has a different origin, and so we leave explicit consideration of this correction for future work.

C. Effect of excluded modes: thermal expansion

Finally, we consider the original decision to reduce the number of degrees of freedom in the effective Hamiltonian to one vector degree of freedom per cell to represent ferroelectric distortions. Even if an optimal set of local-mode variables is chosen (Sec. V A) and all necessary terms in the Taylor expansion are kept (Sec. V B), there still may be errors associated with this fundamental approximation. For example, anharmonic couplings between included and excluded modes are neglected, as are anharmonic couplings between excluded modes and of excluded modes to strain.

The effects of neglecting these anharmonic couplings are clearly seen in the thermal expansion. In fact, in raising the temperature from 0 to 300 K in our simulations, we find that

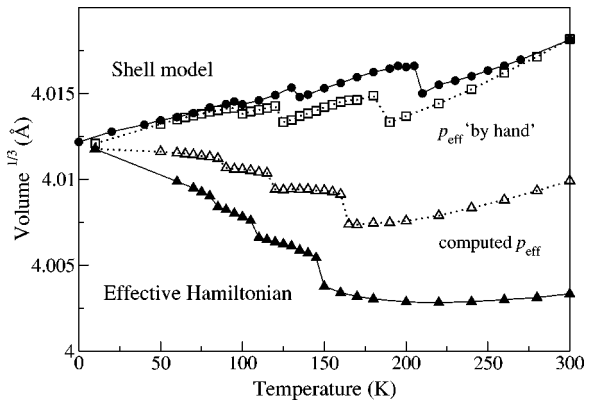

FIG. 2. Pseudocubic lattice parameter $a=V^{1/3}$ (V = cell volume) for $BaTiO_3$ as a function of the temperature as predicted by the effective Hamiltonian (full triangles) and by the shell model (full circles). Open squares and triangles correspond to effective Hamiltonian results under an external pressure adjusted ''by hand'' and *ab initio*, respectively (see text for details).

the volume of the shell-model system *increases* by 0.4%, while that of the effective-Hamiltonian system *decreases* by 0.6%. This indicates that the effective Hamiltonian treatment of the thermal expansion is qualitatively incorrect. Moreover, given the well-known sensitivities of the transition temperatures to volume, this effect could be substantial. Moreover, it correctly predicts that we would underestimate transition temperatures, since they are reduced at smaller lattice constants.

To check whether the thermal expansion effect is responsible for the dominant errors in T_c, we made the following test. We completely eliminated the volume effect by carrying out both simulations at a *fixed volume* of $(4.012\ \text{Å})^3$ while allowing the strain tensor to change. Using the shell model, we have found T_c values of 190, 130, and 95 K, while the corresponding effective-Hamiltonian values are 180, 125, and 100 K, respectively. The error in the $C-T$ transition temperature, which was around 60 K in the zero-pressure simulations, is reduced to ~ 10 K.

D. Summary

We thus arrive at the important conclusion that the poor description of thermal expansion effects is the dominant source of error in the effective-Hamiltonian description. These shortcomings in the description of thermal expansion, and some preliminary attempts to correct for them, will be described in the following section. Smaller errors (probably amounting to no more than 5–10 % of the T_c values) are associated with the other approximations discussed in Secs. V A and V B.

VI. IMPROVED TREATMENT OF THERMAL EXPANSION

Given the conclusion of Sec. V D, we are strongly motivated to improve the effective-Hamiltonian treatment of thermal expansion. First, we investigate the thermal expansion in more detail. Figure 2 shows the pseudocubic lattice parameter $a=V^{1/3}$ as a function of temperature as predicted by the shell model (full circles) and by the effective Hamiltonian (full triangles). Both models exhibit volume anomalies (''kinks'') at the ferroelectric phase transition temperatures, indicative of their first-order character. However, the overall trends in volume vs temperature are quite different.

The thermal expansion displayed by the shell model, after a proper rescaling of temperature and cell parameter, closely resembles that of real $BaTiO_3$.[22] This virtue of the model is related to the fact that it includes all the degrees of freedom of the system and a sufficiently accurate description of their relevant anharmonicities. The effective Hamiltonian, on the other hand, does not properly account for the thermal expansion of the system, and actually leads to a *contraction* with increasing temperature in the range of the polar phases. The reason for such a contraction is that the volume is strongly coupled to the magnitude of the local dipoles and, as these tend to *decrease* with increasing temperature as the paraelectric phase is approached, the volume tends to decrease as well. Equivalently, the thermal contraction can be attributed to negative Grüneisen parameters associated with portions of the relevant branches; these are overwhelmed by positive contributions from higher modes in the shell-model system, but not in the effective-Hamiltonian system where the higher modes are absent.

We next ask what happens if the effective-Hamiltonian simulations are carried out with a cell volume that is constrained ''by hand'' to have the correct dependence on temperature as given by the shell-model system. A simple way of doing this in practice is to apply a (negative) external pressure $p_{\rm eff}$ to the effective-Hamiltonian system (technically, this is done by adding a $p_{\rm eff}V$ term to the effective Hamiltonian). This fictitious pressure can be thought of as arising from the thermal expansion effects of the excluded modes. We implement this approximately by taking $p_{\rm eff}$ to be linear in temperature in such a way that the effective-Hamiltonian equilibrium volume coincides with the shell-model one at two temperatures, taken to be 10 and 300 K, bracketing the relevant range. We then find that $p_{\rm eff}$ is required to be -1.8 GPa at 300 K while almost vanishing at 10 K.[23] The results of MC simulations under this external pressure are presented in Fig. 2 (open squares); the values of the transition temperatures are listed in Table II. The agreement with the shell-model calculations, in particular in the case of the $C-T$ transition temperature, is markedly improved.

However, such an *ad hoc* approach is not consistent with the spirit of first-principles based approaches; one would prefer a way to calculate the effective pressure $p_{\rm eff}$ *ab initio*. We have attempted to do so by employing the so-called quasiharmonic approximation (see Chap. 25 of Ref. 24). Within this approximation, the pressure that develops in a harmonic crystal with volume-dependent phonon frequencies is [see Eq. (25.5) of Ref. 24]

$$p=-\frac{\partial}{\partial V}\left(U^{\rm eq}+\sum_{\mathbf{k}s}\frac{1}{2}\hbar w_s(\mathbf{k})\right)+\sum_{\mathbf{k}s}\left(-\frac{\partial[\hbar w_s(\mathbf{k})]}{\partial V}\right)\frac{1}{e^{\beta\hbar w_s(\mathbf{k})}-1}, \tag{3}$$

where U^{eq} is the equilibrium energy of the system, $\omega_s(\mathbf{k})$ is the phonon frequency of branch s at point $\mathbf{k}$ of the Brillouin zone (BZ), and the summations run over all branches and $\mathbf{k}$ points. Now the pressure exerted by the excluded modes is obtained from Eq. (3) by removing U^{eq} and restricting the sums to the excluded modes s'. Taking the classical limit $\hbar \to 0$ in order to compare with the classical shell model, p_{eff} takes the form

$$p_{\mathrm{eff}} = k_B T \frac{\partial}{\partial V} \left(\sum_{\mathbf{k}s'} \ln \omega_{s'}(\mathbf{k}) \right) \tag{4}$$

which is linear in temperature and proportional to the volume derivative of the phonon frequencies.

We must be cautious about the approximations involved in the use of Eq. (4) or its quantum-mechanical version. The quasiharmonic approach is not really well suited to deal with phase transitions, which are strongly anharmonic phenomena. Using it in the present context relies on the assumption that the excluded modes (more precisely, the volume derivatives of their frequencies) are not significantly affected by the strong fluctuations and phase transitions associated with the relevant local modes.

In order to assess the utility of the quasiharmonic approach here, we have focused on the cubic-to-tetragonal transition and calculated p_{eff} using the volume dependences of the excluded-mode frequencies in the cubic paraelectric phase.[25] We find that the BZ sum in Eq. (4) can be evaluated with good accuracy using information from the high-symmetry k points only, and that the sum of logarithms of the hard-mode frequencies depends linearly with volume in the relevant volume range, thus allowing us to take p_{eff} as independent of volume. The p_{eff} calculated in this way shows improved agreement with the exact shell-model results as regards both the transition temperatures (denoted by ''computed p_{eff}'' in Table II) and the thermal expansion (open triangles in Fig. 2). Note that p_{eff} is equal to -0.86 GPa at 300 K, approximately one half of the value that corresponds to the correction ''by hand.'' The results are still far from satisfactory, with a substantial error remaining for the $C-T$ transition temperature. These discrepancies are probably connected with the shortcomings of the quasiharmonic approximation discussed above. Further investigations along these lines are clearly needed, but fall beyond the scope of the present paper.

In summary, the proposed correction based on the quasiharmonic approximation of Eq. (4) accounts correctly for only a fraction (perhaps a third) of the thermal-expansion error. Unfortunately, then, we are not yet in a position to propose a fully *ab initio* approach to the thermal expansion problem in the context of effective-Hamiltonian methods.

VII. CONCLUSIONS

The main weakness of our effective-Hamiltonian description of shell-model $BaTiO_3$ is the poor description of the thermal expansion. Focusing on the cubic to tetragonal transition temperature (T_{CT}), we have found that the effective Hamiltonian produces a 28% error, while we can estimate from our constant-volume calculations that this error should be reduced to 5% if the thermal expansion were properly modeled. We have also seen that including the thermal expansion ''by hand'' allows us to reduce the error to about 12%; in other words, this correction seems to account for 70% of the total error associated with the thermal expansion.

It is tempting to apply these same percentages in order to estimate the sources of error arising in the comparison of the first-principles effective Hamiltonian transition temperatures with real experiment. However, this should be done cautiously. For example, anharmonicities or thermal-expansion effects might either be exaggerated or underestimated by the shell model. With this in mind, we consider the effective-Hamiltonian study of $BaTiO_3$ by Zhong *et al.* which led to $T_{CT}=300$ K, 25% below the experimental value of 400 K. This was a classical calculation; should quantum effects be considered, the calculated T_{CT} would be smaller by about 30 K,[12] and thus the error would go up to $\sim 30\%$.

We performed classical MC simulations with the effective Hamiltonian of Zhong *et al.* including the thermal expansion of the system ''by hand'' under the condition that the computed volume should coincide with the experimental one at $T=473$ K. This resulted in an error of 18% in T_{CT}, which would become $\sim 25\%$ if we include the estimated quantum effects. Hence, it seems that the improvement in this case is not as large as it was for the effective Hamiltonian fitted to shell-model $BaTiO_3$. If we follow what we have learned from the case of shell-model $BaTiO_3$ and assume that including the thermal expansion ''by hand'' corrects 70% of the total thermal-expansion error, we can estimate that a quantum first-principles effective-Hamiltonian calculation with perfect thermal expansion would still result in a 20% underestimate of T_{CT}. It seems reasonable to assume that type II errors other than the thermal expansion, as well as details of the fitting procedure, are responsible for a further 5% error in T_{CT}. This suggests that a calculation free of type II and IV errors would yield a T_{CT} that would still be about 15% below experiment. While this line of reasoning is tenuous, we nevertheless believe it gives the best current estimate for the magnitude of the error that should be attributed to the first-principles methods used to construct the effective Hamiltonian (in particular, the LDA).

In summary, in this work we have analyzed the errors associated with the first-principles effective Hamiltonian method that has been developed for the treatment of the thermodynamics of perovskite ferroelectrics. More specifically, by considering the effective-Hamiltonian description of the shell-model for $BaTiO_3$ of Tinte *et al.*, we have been able to isolate and study in detail the errors intrinsic to the effective-Hamiltonian approximation (type II errors). We have found that the main type II error is associated with a poor description of the thermal expansion of the system. We have discussed an easily implemented first-principles correction that takes into account some contributions of excluded modes. Unfortunately, this scheme seems to account for only about a third of the total thermal-expansion error. More elaborate schemes (involving a more thorough treatment of the couplings of the phonon modes to each other and to strain and polarization) might substantially reduce the error, but it re-

mains for the future to explore and implement such schemes. Finally, we have argued that in the case of the comparison of the first-principles effective-Hamiltonian calculations on $BaTiO_3$ with real experiment, type II errors do not seem to be responsible for the entire discrepancy. Our results suggest that the type I errors associated with the use of the LDA and other first-principles technicalities may be of the same magnitude as the thermal-expansion error.

ACKNOWLEDGMENT

This work was supported by the Center for Piezoelectrics by Design (CPD) under ONR Grant No. N00014-01-1-0365. Computational facilities for the work were also provided by the CPD. J.I. acknowledges the financial support of ONR Grant No. N0014-97-1-0048.

[1] For a review and list of references see D. Vanderbilt, Curr. Opin. Solid State Mater. Sci. **2**, 701 (1997).
[2] W. Zhong, D. Vanderbilt, and K.M. Rabe, Phys. Rev. Lett. **73**, 1861 (1994).
[3] W. Zhong, D. Vanderbilt, and K.M. Rabe, Phys. Rev. B **52**, 6301 (1995).
[4] S. Tinte, M.G. Stachiotti, M. Sepliarsky, R.L. Migoni, and C.O. Rodríguez, J. Phys.: Condens. Matter **11**, 9679 (1999).
[5] U.V. Waghmare and K.M. Rabe, Phys. Rev. B **55**, 6161 (1997).
[6] M. Sepliarsky, M.G. Stachiotti, and R.L. Migoni, Phys. Rev. B **56**, 566 (1997).
[7] H. Krakauer, R. Yu, C.-Z. Wang, K.M. Rabe, and U.V. Waghmare, J. Phys.: Condens. Matter **11**, 3779 (1999).
[8] L. Bellaiche, A. García, and D. Vanderbilt, Phys. Rev. Lett. **84**, 5427 (2000).
[9] K. Leung, E. Cockayne, and A.F. Wright, Phys. Rev. B **65**, 214111 (2002).
[10] R. Hemphill, L. Bellaiche, A. García, and D. Vanderbilt, Appl. Phys. Lett. **77**, 3642 (2001).
[11] M. Sepliarsky, S.R. Phillpot, M.G. Stachiotti, and R.L. Migoni, J. Appl. Phys. **91**, 3165 (2002).
[12] J. Íñiguez and D. Vanderbilt, Phys. Rev. Lett. **89**, 115503 (2002).
[13] S. Tinte, M.G. Stachiotti, C.O. Rodríguez, D.L. Novikov, and N.E. Christensen, Phys. Rev. B **58**, 11 959 (1998).
[14] R. Migoni, H. Bilz, and D. Bäuerle, Phys. Rev. Lett. **37**, 1155 (1976).
[15] G.V. Lewis and C.R.A. Catlow, J. Phys. C **18**, 1149 (1985).
[16] DL-POLY is a package of molecular simulation routines written by W. Smith and T. R. Forester, Daresbury and Rutherford Appleton Laboratory, Daresbury, UK.
[17] K.M. Rabe and U.V. Waghmare, Phys. Rev. B **52**, 13 236 (1995).
[18] For convenience, we use the terms ''phonons'' or ''normal modes'' to refer to the eigenvectors of the force-constant matrix.
[19] J. Íñiguez, A. García, and J.M. Perez-Mato, Phys. Rev. B **61**, 3127 (2000).
[20] When the simulations are performed decreasing the temperature, we find the same transition sequence with hysteresis in T_c's of less than 5 K.
[21] This approximation is known to be inappropriate for some systems. For example, the authors of Ref. 9 found that nonlocal anharmonic couplings involving oxygen octahedron tilting variables are essential to reproduce the experimentally observed phase diagram of Zr-rich PZT.
[22] G. Shirane and A. Takeda, J. Phys. Soc. Jpn. **7**, 1 (1952).
[23] Leung *et al.* (Ref. 9) also considered an effective pressure varying linearly with temperature in order to incorporate thermal expansion in their effective-Hamiltonian study of Zr-rich PZT. Interestingly, the coefficient they used (-5.56 MPa/K) is very similar to the one that corresponds to the shell model of $BaTiO_3$ (-6.21 MPa/K).
[24] N. W. Ashcroft and N. D. Mermin, *Solid State Physics* (Saunders College Publishing, Philadelphia, 1976).
[25] One could think of computing p_{eff} for each of the phases of the system, which should then be treated separately in the simulation.